Sensors and Materials, Vol. 16, No. 5 (2004) 231–239
MYU Tokyo

S & M 0561

Preparation of $PbSc_{0.5}Ta_{0.5}O_3$ Ferroelectric Thin Films For Infrared Detection by Pulsed Laser Deposition

Shuichi Murakami*, Daniel Popovici[1], Kazuo Satoh, Mitsuteru Matsumoto, Minoru Noda[1] and Masanori Okuyama[1]

Technology Research Institute of Osaka Prefecture,
2-7-1 Ayumino Izumi, Osaka 594-1157, Japan
[1] Graduate School of Engineering Science, Osaka University,
1-3 Machikaneyama-cho, Toyonaka, Osaka 560-8531, Japan

(Received April 7, 2004; accepted August 4, 2004)

Key words: ferroelectric thin film, $PbSc_{0.5}Ta_{0.5}O_3$, infrared sensor of dielectric bolometer mode

Preferentially (222)-oriented $PbSc_{0.5}Ta_{0.5}O_3$ (PST) thin films were prepared on Pt/Ti/SiO_2/Si substrates by pulsed laser deposition at a temperature as low as 400°C. Their ferroelectric properties were improved by postdeposition annealing at 500°C, where the polarization at zero electric field was 1.4 μC/cm^2. The temperature coefficient of the dielectric constant (TCD) was also improved to 1.1%/K at 25°C, indicating that the PST thin film is a promising candidate material for use in an infrared image sensor of dielectric bolometer mode, which is based on the temperature dependence of the dielectric constant.

1. Introduction

In recent years uncooled thermal infrared (IR) sensors of dielectric bolometer (DB) mode have attracted much attention,[1–3] because they operate with high sensitivity, without chopping, at low power and at room temperature. In the IR sensor of DB mode, the dielectric constant change with temperature is detected through the capacitance change in a ferroelectric thin film such as $(Ba_{1-x}Sr_x)TiO_3$ (BST),[4,5] $Ba(Ti_{1-x}Sn_x)O_3$ (BTS),[6,7] $Pb(Mg_{1-x}Nb_x)O_3$-$PbTiO_3$ (PMN-PT) or $(Sr_{1-x}Ba_x)Nb_2O_6$ (SBN).[8] To obtain a high figure of merit for voltage responsivity (R_v) and specific detectivity (D^*), it is advantageous for the ferroelectric thin film to have a Curie temperature (T_c) close to the operating temperature.

*Corresponding author, e-mail address: sh-murakami@tri.pref.osaka.jp

We have so far reported on BST and BTS films as IR detecting ferroelectric materials in the IR sensor of DB mode, for which a high figure of merit was obtained, and some 2D array sensors have been demonstrated.[4–8] However, a BST film having high sensitivity showed low resistivity, and a film having high insulation showed low sensitivity. Consequently, it was difficult to obtain good performance with high reliability, reproducibility and stability.

Solid-solution $Pb(Sc_{0.5}Ta_{0.5})O_3$ (PST) in a complex perovskite structure ($A(B'B'')O_3$) is another attractive candidate material for fabricating an IR sensor of DB mode. Because bulk PST exhibits a first-order phase transition over the temperature range from 0 to 26°C,[9] a PST thin film is expected to show a high temperature coefficient of dielectric constant (TCD) around room temperature. PST films have been grown by sputtering,[10,11] sol-gel,[12] metal-organic chemical vapor deposition[13] and pulsed laser deposition (PLD).[14] However, few reports have appeared concerning PST deposition on $Pt/Ti/SiO_2/Si$ substrates, on which we have previously developed monolithic integration of a detecting capacitor, signal-processing MOSFETs and a thermally insulated structure for a detector pixel using Si bulk micromachining.[15]

In this study, we report first on a preferentially (222)-oriented PST film prepared on a $Pt/Ti/SiO_2/Si$ substrate by PLD with a low deposition temperature. Next, by optimizing the postdeposition annealing conditions, we investigated how to improve the ferroelectricity and TCD from the viewpoint of applications to IR sensors of DB mode.

2. Experimental

An ArF excimer laser (wavelength: 193 nm) was used for ablation. The laser beam was focused with a quartz lens onto a $Pb_{1.2}Sc_{0.5}Ta_{0.5}O_3$ ceramic target rotating in a vacuum chamber. Deposition conditions are shown in Table 1. The substrate was $Pt/Ti/SiO_2/Si(100)$, on which metal layers (20-nm-thick Ti and 200-nm-thick Pt) were successively deposited by RF magnetron sputtering on a thermally oxidized Si(100) wafer. The

Table 1
Conditions of deposition and postdeposition annealing of PST films by pulsed laser deposition.

Target	PST ceramic disk
Substrate	$Pt/Ti/SiO_2/Si(100)$
Substrate temperature	300–600°C
Gas	O_2
Gas pressure	27 Pa
Laser	ArF excimer
Repetition frequency	5 Hz
Fluency	1.5 J/cm^2
Target-substrate distance	30 mm
Deposition time	4 h
Postdeposition annealing temperature	400–800°C
Postdeposition annealing time	1–30 min

chamber was evacuated to a pressure below 10^{-5} Pa before O_2 gas was introduced. The deposition was performed for 4 h, and the deposited film thickness was 300 nm. The films were postdeposition annealed over a temperature range of 400 to 800°C in flowing oxygen. To fabricate metal-ferroelectric-metal capacitors, the top Pt electrode was deposited on the PST film by RF magnetron sputtering. The area of the top electrode was 8.0×10^{-4} cm^2.

Crystalline structures of the deposited films were analyzed by X-ray diffraction (XRD) analysis (RINT-2000), and a scanning electron microscope (SEM) was used to observe the film surface morphology. Polarization hysteresis and leakage current were evaluated using a ferroelectric test system (TOYO Corporation). The dielectric constant and loss value were measured using an LCR meter at 1 kHz and 1 V over a temperature range of 20 to 50°C.

3. Results and Discussion

3.1 *Crystallization characteristics*

The XRD patterns of the as-deposited PST films on Pt/Ti/SiO_2/Si(100) as a function of deposition temperature are shown in Fig. 1. As shown in this figure, film crystallinity depends strongly on the deposition temperature. The PST film deposited at 300°C has an amorphous structure. On the other hand, a predominant peak corresponding to the pyrochlore phase of PST (pyr(222)) was detected for the PST films deposited in the temperature range over 450°C. Only the PST film deposited at 400°C shows the preferred PST perovskite orientation (per(222)).

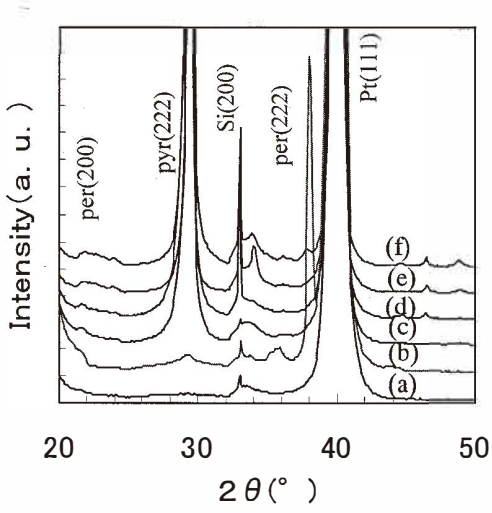

Fig. 1. XRD patterns of PST films on Pt/Ti/SiO_2/Si substrate as a function of substrate temperature during deposition: (a) 300°C, (b) 400°C, (c) 450°C, (d) 500°C, (e) 550°C, (f) 600°C.

First, we tried to obtain the PST perovskite structure in the film deposited at 300°C by postdeposition annealing at a temperature of 800°C, and investigated the crystallization characteristics of the PST films and the thermal stability of the pyrochlore and perovskite phases of PST. Figure 2 shows the XRD patterns for the 300°C-deposited films as a function of postdeposition annealing temperature. The XRD patterns reveal that the PST pyrochlore (222) peak intensity increases as the postdeposition annealing time increases, and that the PST perovskite (222) peak is observed only for 1 min postdeposition annealed PST films. It becomes clear that the amorphous PST films deposited at 300°C are prone to transformation to the PST pyrochlore phase rather than the perovskite phase by postdeposition annealing. Furthermore, the PST films deposited over 450°C, which showed preferentially (222)-oriented pyrochlore structures, as shown in Fig. 1, could not be transformed to the PST perovskite structure by postdeposition annealing at temperatures of 700 and 800°C.

In this study, we focus on the PST films deposited at 400°C, because these films have the preferentially (222)-oriented perovskite structure but little pyrochlore structure, as shown in Fig. 1. The 400°C-deposited PST films, however, have a small ferroelectricity, as is shown in Fig. 4. Therefore, we investigate the effect of postdeposition annealing on improving ferroelectricity. The PST films were postdeposition annealed for 30 min, which is considered to be long enough to change the crystallinities of the films from those shown in Fig. 2. Figure 3 shows the XRD patterns of the PST films deposited at 400°C as a function of postdeposition annealing temperature. The XRD patterns reveal that the PST pyrochlore (222) peak intensity increases slightly as the postdeposition annealing temperature increases. In contrast, the PST perovskite (222) peak intensities are almost the same at the postdeposition annealing temperatures of 400 and 500°C, while the peak disappears at a postdeposition annealing temperature above 550°C.

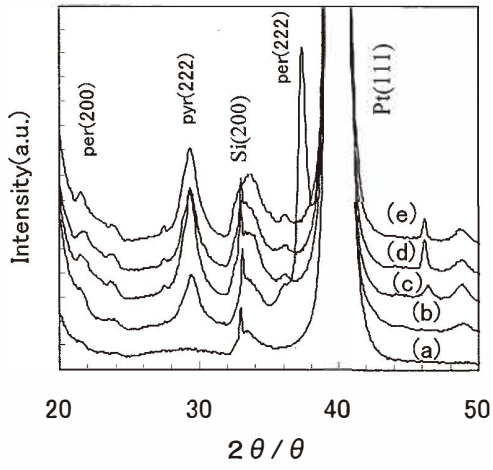

Fig. 2. XRD patterns of PST films deposited at 300°C on Pt/Ti/SiO_2/Si substrate as a function of postdeposition annealing time: (a) as-deposited, (b) 1 min, (c) 3 min, (d) 10 min, (e) 30 min.

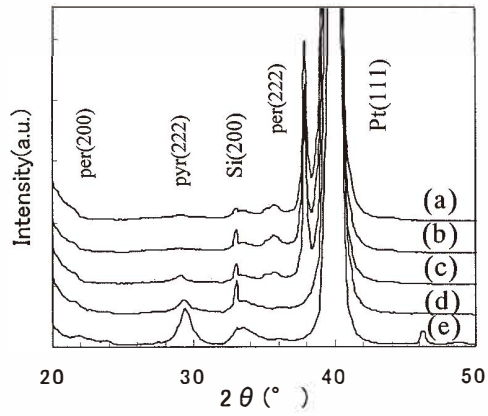

Fig. 3. XRD patterns of PST films on Pt/Ti/SiO_2/Si substrate as a function of postdeposition annealing temperature: (a) as-deposited, (b) 400°C, (c) 500°C, (d) 550°C, (e) 800°C.

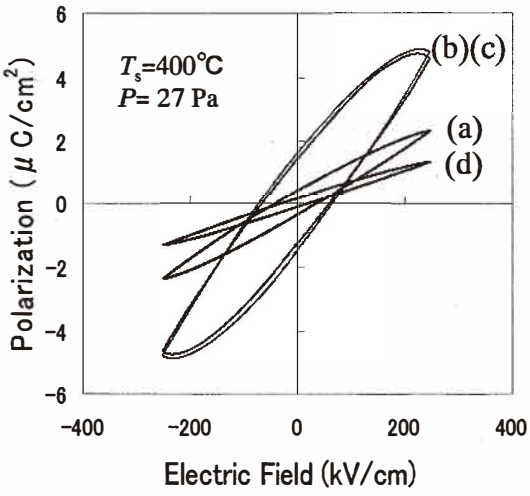

Fig. 4. *P-E* hysteresis loops of 400°C-deposited PST films at different postdeposition annealing temperatures: (a) as-deposited, (b) 400°C, (c) 500°C, (d) 550°C.

3.2 *Effect of postdeposition annealing on electric properties and surface morphology*

Figure 4 shows the *P-E* hysteresis loops at room temperature (25°C) for PST films deposited at 400°C before and after postdeposition annealing at temperatures of 400 to 550°C. The as-deposited PST film shows a small ferroelectricity with a polarization of 0.5 μC/cm^2 at zero electric field, and the 400°C- and 500°C-postdeposition annealed PST films exhibit improved ferroelectricity with a polarization of 1.4 μC/cm^2 at zero electric field, which is three times larger than that of the as-deposited PST films.

On the other hand, the PST films which were annealed above 550°C show almost no ferroelectricity. This phenomenon is consistent with the experimental result that the 550°C-postdeposition annealed PST film does not exhibit the PST perovskite (222) peak, as can be seen in Fig. 3.

It is interesting to note that the ferroelectricity of the PST film was improved by postdeposition annealing at 400 and 500°C, whereas the PST perovskite (222) peak intensities of the PST films are almost the same before and after postdeposition annealing. Thus, we investigate the influence of postdeposition annealing at 500°C on surface morphology, leakage characteristics and dielectric constant to clarify the reason for the improvement of the ferroelectricity.

Figure 5 shows SEM images of surface morphology of the 400°C-deposited PST films before and after postdeposition annealing at 500°C. As can be seen in the figure, both films consist of spherical grains and little pores exist between the grains. There was no considerable change before and after postdeposition annealing. The grain size is approximately 50 nm, which is much smaller than the reported grain size of bulk PST (about 2–8 μm).[16]

Figure 6 shows the leakage current characteristics at room temperature (25°C) for PST films before and after postdeposition annealing at 500°C. It is found from the figure that the leakage currents of both films are relatively small and that there is not remarkable change induced by postdeposition annealing.

Figure 7 shows the temperature dependence of the relative dielectric constant of the PST films before and after postdeposition annealing at 500°C. It is found from this figure

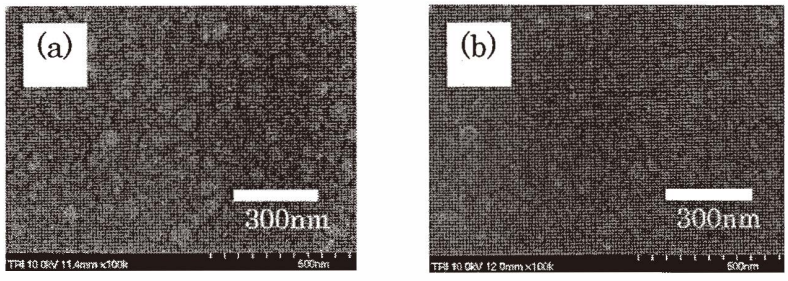

Fig. 5. SEM images of PST films (a) before and (b) after postdeposition annealing at 500°C.

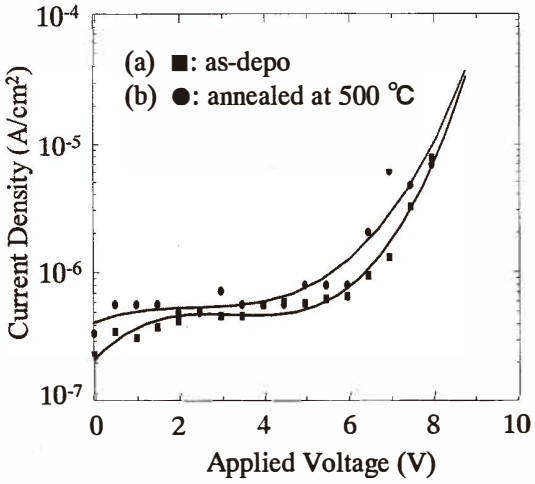

Fig. 6. Current density vs. applied voltage for PST films (a) before and (b) after postdeposition annealing at 500°C.

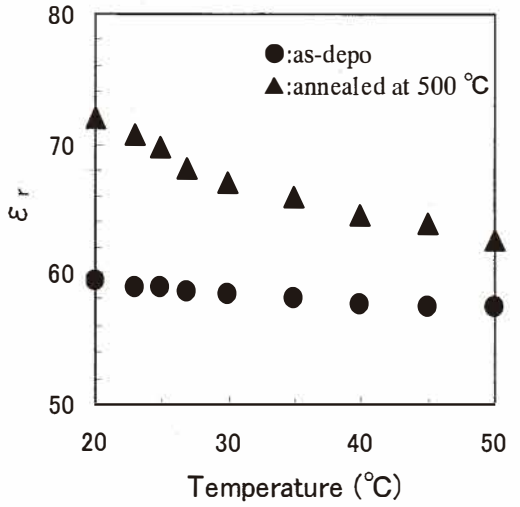

Fig. 7. Temperature dependence of dielectric constant of PST films before and after postdeposition annealing at 500°C.

that the dielectric constants of both films decrease monotonically as temperature increases.

The temperature dependence of the dielectric constant is relatively broad, which is different from the sharp change in dielectric constant observed in bulk PST ferroelec-

trics.[14] This phenomenon is explained in the framework of diffuse phase transition behavior.[17] Moreover, the relative dielectric constants of both films are much smaller than the bulk ferroelectrics, because the grain size of the films is two orders of magnitude smaller than that of the bulk ferroelectrics.[16]

Compared to the as-deposited PST film, the 500°C-postdeposition annealed film shows a sharper temperature dependence of the dielectric constant. It is interesting to note that this is consistent with an improvement in the *P-E* hysteresis loop by postdeposition annealing as can be seen in Fig. 4.

From these experimental results, the postdeposition annealing at 500°C does not affect the improvement of crystalline properties, surface morphology and leakage characteristics. However, the ferroelectric property is greatly improved, and the TCD becomes sharper after postdeposition annealing. This phenomenon is considered to be due to the improvement in the domain structure, in the contact between the bottom electrode and the PST film, or the enhancement of the degree of order for B-site cations (Sc^{3+}, Ta^{5+}).[12] The detailed mechanism is currently under consideration.

3.3 *Temperature coefficient of dielectric constant*

Applied to the infrared (IR) sensor of dielectric bolometer (DB) mode, it is important for the film to exhibit a high TCD at room temperature. TCD is expressed as

$$TCD = \frac{1}{\varepsilon_r}\frac{d\varepsilon_r}{dT} \times 100(\%/K), \tag{1}$$

where ε_r is the relative dielectric constant and T is the temperature. The TCDs of the PST films before and after postdeposition annealing at 500°C are determined as 0.18 and 1.1%/K (at 25°C), respectively. The TCD of the postdeposition annealed PST film is high enough to make it possible to apply for human-body detection. Furthermore, the dielectric loss is as low as about 0.04–0.07 at 1 kHz and 1 V in the temperature range of 20 to 50°C. Therefore, it is concluded that the PST film is a good candidate material for use in an IR sensor of DB mode.

4. Conclusions

The PST films were prepared on Pt/Ti/SiO_2/Si(100) substrates by pulsed laser deposition. The deposition temperature is the principle factor in obtaining a high crystalline PST perovskite structure, and the PST film has the preferentially (222)-oriented perovskite structure but little pyrochlore structure when deposited at 400°C. The ferroelectricity and TCD were improved by postdeposition annealing at temperatures of 400 and 500°C, whereas little change was observed in the crystalline property, surface morphology and leakage characteristics. It is interesting to note that the perovskite phase and ferroelectricity disappear simultaneously due to postdeposition annealing in the temperature range above 550°C.

The PST film, which was deposited at 400°C and postdeposition annealed at 500°C, shows a ferroelectricity with a polarization of 1.4 μC/cm^2 at zero electric field. The grain size was approximately 50 nm, and the leakage currents of both films were relatively small. The dielectric constant decreases monotonically with increasing temperature from 20 to 50°C. The TCD is 1.1%/K at 25°C, implying that the film is a promising candidate material for use in infrared sensors of dielectric bolometer mode.

References

1 J. F. Belcher, C. M. Hanson, H. R. Beratan, K. R. Udayakumar and K. L. Soch: Infrared Technology and Applications XXIV **3436** (1998) 612.
2 M. Noda, K. Hashimoto, R. Kubo, H. Tanaka, T. Mukaigawa, H. Xu and M. Okuyama: Sens. Actuators, A **77** (1999) 39.
3 M. A. Todd, P. A. Manning, P. P. Donohue, A. G. Brown and R. Watton: Infrared Technology and Applications XXVI **4130** (2000) 128.
4 H. Zhu, M. Noda, T. Mukaigawa, H. Xu, K. Hashimoto and M. Okuyama: T. IEEE Japan **120-E** (2000) 554.
5 M. Noda, K. Inoue, M. Ogura, H. Xu, S. Murakami, H. Kishihara and M. Okuyama: Transducers '01 (Munich, Germany, 2001) p. 564.
6 T. Miyamoto, S. Murakami, K. Inoue, Y. Suzuki, T. Nomura, M. Noda and M. Okuyama: 13th IEEE Int. Symp. on the Application of Ferroelectrics (2002) p. 191.
7 M. Noda, T. Nomura, D. Popovici, Y. Kuwahara, S. Murakami and M. Okuyama: Proc. of the 20th Sensor Symposium (2003) p. 199.
8 K. Hashimoto, H. Xu, T. Mukaigawa, R. Kubo, H. Zhu, M. Noda and M. Okuyama: Sens. Actuators, A **88** (2001) 10.
9 P. P. Donohue, M. A. Todd, C. J. Anthony, A. G. Brown, M. A. C. Harper and R. Watton: Integrated Ferroelectrics **41** (2001) 25.
10 I. M. Reaney, D. J. Barber and R. Watton: J. Mater. Sci. **3** (1992) 51.
11 M. A. Todd, P. P. Donohue, J. C. Jones, D. J. Wallis, M. J. Slater, M. A. Harper and R. Watton: Integrated Ferroelectrics **25** (1999) 113.
12 D. Liu and D. A. Payne: J. Appl. Phys. **77** (1995) 3361.
13 C. H. Lin, S. W. Lee and H. Chen: Appl. Phys. Lett. **75** (1999) 2485.
14 C. Bjormander, K. Sreenivas, A. M. Grishin and K. V. Rao: Appl. Phys. Lett. **67** (1995) 58.